ELSEVIER

International Journal of Mass Spectrometry 220 (2002) 343–357

International Journal of Mass Spectrometry

www.elsevier.com/locate/ijms

Excited-state proton transfer in naphthol/solvent clusters: the current state of affairs

Richard Knochenmuss[a,1], Ingo Fischer[b,*]

[a] *OC, D-CHEM, ETH Zürich, CH-8093 Zürich, Switzerland*
[b] *Institut für Physikalische Chemie, Universität Würzburg, Am Hubland, D-97074 Würzburg, Germany*

Received 11 January 2002; accepted 18 March 2002

Abstract

Excited-state proton transfer (ESPT) in naphthol/solvent clusters is among the best studied intracluster-reactions. In this paper, we summarize the experimental results obtained for one of the most important cluster ESPT systems: 1-naphthol/ammonia. A particularly wide range of techniques has been applied to this system, including laser-induced fluorescence, [1 + 1] and [1 + 1′] multiphoton ionization, and time-resolved photoionization. The data are discussed within the framework of existing models for ESPT and compared to 1-naphthol/water clusters as well as to clusters of the related chromophores 2-naphthol and 5-cyano-2-naphthol. While ESPT in clusters with nitrogen bases can be described by an adiabatic model, with proton transfer proceeding on a single electronic surface, ESPT in water clusters has to be described by a non-adiabatic model, in which a solvent-induced post-excitation mixing of the L_a and L_b states of the bare naphthols due to vibronic coupling is responsible for the proton transfer reaction. (Int J Mass Spectrom 220 (2002) 343–357)

1. Introduction

Intermolecular excited-state proton transfer (ESPT) of naphthol to various solvents is among the most extensively studied dynamical processes in clusters. In this reaction, the aromatic naphthol chromophore (NpOH) is photoexcited, and then donates a proton in the excited state to a solvent molecule (M), forming a solvated, charge-separated ion pair.

$$\text{1-NpOH(M)}_n \rightarrow [\text{1-NpOH(M)}_n]^* \rightarrow \text{1-NpO}^-(\text{MH}^+)(\text{M})_{n-1} \quad (1)$$

To understand why this reaction is of such high interest, one has to consider the motivations for studying clusters in general:

- By studying the properties of clusters as a function of size it is possible to make a connection between single-molecule, few-molecule and condensed-phase behavior [1]. Using the well-defined conditions of a supersonic molecular beam, clusters thereby offer the opportunity to study phenomena present in the condensed phase, but in a more detailed manner.
- Clusters are held together by weak non-covalent forces, and thus make it possible to examine these bonds in detail [2]. The most important non-covalent interaction is certainly the hydrogen bond,

* Corresponding author.
E-mail: ingo@phys-chemie.uni-wuerzburg.de
[1] Co-corresponding author.
E-mail: knochenmuss@org.chem.ethz.ch

1387-3806/02/$ – see front matter
PII S1387-3806(02)00687-5

since the three-dimensional structure of many biomolecules relies on it. Studies of hydrogen-bonded clusters can thus contribute to a better theoretical description of weak bonds in complex molecules [3–5]. This includes not only static effects related to structure, but also dynamic effects determining reactivity.

- While details of unimolecular reactions are best obtained from isolated molecules, it is difficult to get similarly accurate information on bimolecular reactions. Initiating such reactions in clusters, however, provides an opportunity to learn more about the dynamics of bimolecular reactions [6], while minimizing the complications that come with the usual condensed-phase studies.

Intermolecular proton transfer is perhaps the most important elementary reaction in the condensed phase [7], especially since it is critical for many biological processes. How gas-phase work contributes to our understanding of acid–base reactions in the condensed phase was convincingly demonstrated before [8]. Since in a proton-transfer reaction the making and breaking of hydrogen bonds is involved, one can learn much about the properties of the most important non-covalent bond. In addition, the current level of both theory and experiments has become high enough to yield synergies in developing a detailed description of this bimolecular reaction. Thus, by studying proton transfer reactions one obtains information on all three of the issues mentioned above.

From our point of view the possibility to isolate and study bimolecular reactions under well-defined conditions is the most interesting aspect of intra-cluster chemistry. Only a few bimolecular reactions have been investigated at a similarly detailed level as ESPT, under isolated conditions. The best known is the CO_2–HI system, employed to initiate the reaction CO + OH [9–11].

1-Naphthol was one of the first molecules identified as an excited state acid. When Förster [12] and Weller [13] studied the photochemistry of 1-naphthol in aqueous solution, they observed a strong red-shifted emission over a large pH range in which the ground state

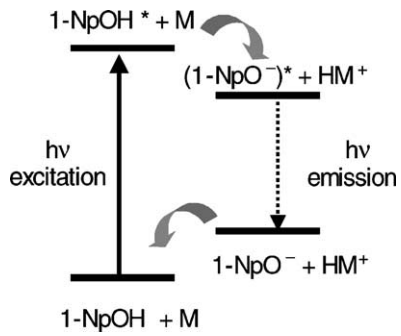

Fig. 1. A schematic representation of excited-state proton transfer, similar to a Förster-diagram. 1-Naphthol is more acidic in its excited electronic state, in aqueous solution proton transfer to the solvent M and formation of the naphtholate anion is energetically favorable. Since the charge separated ground state is energetically higher than the covalent ground state, emission from the naphtholate anion is strongly red-shifted relative to the excitation wavelength.

was not dissociated. By comparison with deprotonated naphthol at high pH, this was assigned as originating from electronically excited naphtholate anions. The process is indicated in Fig. 1. The red-shifted naphtholate emission is still considered to be the major hallmark of ESPT. Photoinduced ESPT can be considered to be a reaction induced by a pH-jump of the system, and is thus, a modern example of a relaxation method, introduced to study the kinetics of fast reactions.

For reasons of experimental convenience and hoped-for simplicity, most of the work on intermolecular cluster ESPT has employed phenol and naphthol reactant chromophores. The 1-NpOH/$(NH_3)_n$ system will be at the center of this review. Its major advantage is the occurrence of ESPT at a relatively small number of solvent molecules, n. This permits not only particularly detailed experiments, but also allows for more accurate calculations. However, we will compare ESPT in 1-NpOH/$(NH_3)_n$ clusters to related systems, like 1-NpOH/$(H_2O)_n$, and also to the ammonia clusters of other naphthols, such as 2-naphthol or 5-cyano-2-naphthol. ESPT in the second important model system, phenol/solvent clusters, has been studied by several groups [14–19]. A discussion of that work is beyond the scope of the present review.

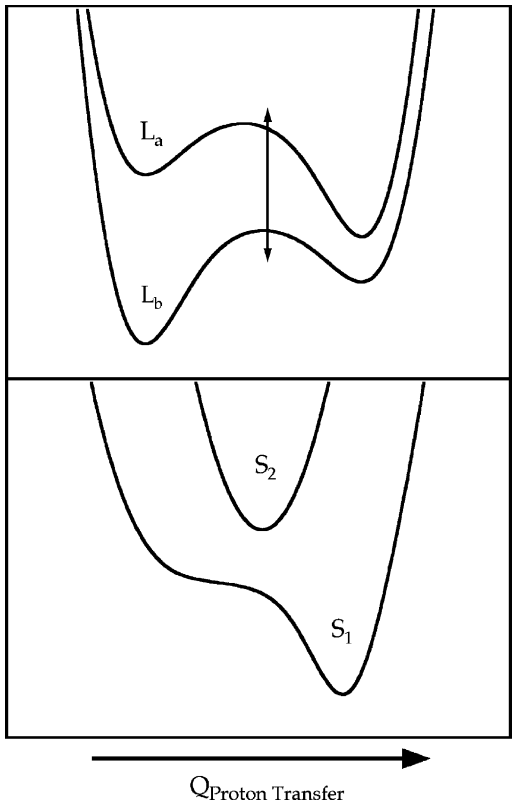

Fig. 2. When the excited electronic states in naphthol initially retain their original character, either L_a or L_b, proton transfer follows a non-adiabatic mechanism (upper trace). However, the relative positions and natures of the states are modulated by vibronic coupling and solvent reorganization. In adiabatic PT (lower trace) the two states are strongly mixed prior to excitation. Proton transfer proceeds on a single surface which is not well described as either L_b to L_a. Reproduced from [58] by permission of Laser Pages Publishing Ltd.

2. Adiabatic vs. non-adiabatic proton transfer

Borgis and Hynes suggested a distinction between adiabatic and non-adiabatic proton transfer reactions [20], as illustrated in Fig. 2. In phenols and naphthols, two close-lying excited state are generally involved in the ESPT process, termed L_a and L_b, the latter generally being energetically lower. The coupling between these naphthalene-like states is mediated by the solvent or by intramolecular motions. If the excited states of the naphthol are (initially) only weakly coupled and largely retain their character, the ESPT process is termed non-adiabatic. Due to various effects to be discussed below the two states will move with respect to each other during the reaction, and become more mixed, or invert, during ESPT.

If, on the other hand, the solvent induces a strong coupling between the reactant excited states *prior to excitation*, two new adiabatic potential energy surfaces are formed. These no longer are well described as only L_a or L_b, and must be more generally denoted as S_1 and S_2 states. The barrier for motion of the proton can, as a result, be low enough for the first vibrational eigenstates to be above the barrier, permitting ESPT to occur spontaneously (i.e. without thermal activation) after excitation. This situation is termed adiabatic ESPT, proceeding on a single surface that changes its character (from L_b- to L_a-like) along the reaction coordinate.

ESPT in 1-NpOH/$(NH_3)_n$ clusters is thought to be an example of such an adiabatic process, while the 1-NpOH/$(H_2O)_n$ system represents a model for non-adiabatic proton transfer. This switching between the two main mechanistic types adds to the interest of 1-NpOH.

Adiabatic ESPT is often discussed in terms of a simplified one-dimensional proton-transfer coordinate. However, one has to be aware that proton transfer is a rather complex reaction. Inspection of Fig. 2 immediately shows that it will always be accompanied by intramolecular vibrational energy redistribution (IVR), and thus, occurs on a multidimensional surface. Since solvation of the charge-separated ion-pair state is the energetic driving force of the reaction, one also expects an extensive rearrangement of the solvent shell during the reaction. These coordinates are seldom included beyond a single generic vibration modulating the potential surfaces. Thus, one has to be aware that one-dimensional models for proton transfer are an often helpful, but nevertheless rather crude approximation.

3. Electronic spectroscopy of 1-NpOH/$(NH_3)_n$ clusters

The first molecular beam studies on ESPT in clusters date back to the late 1980s, when Cheshnovsky

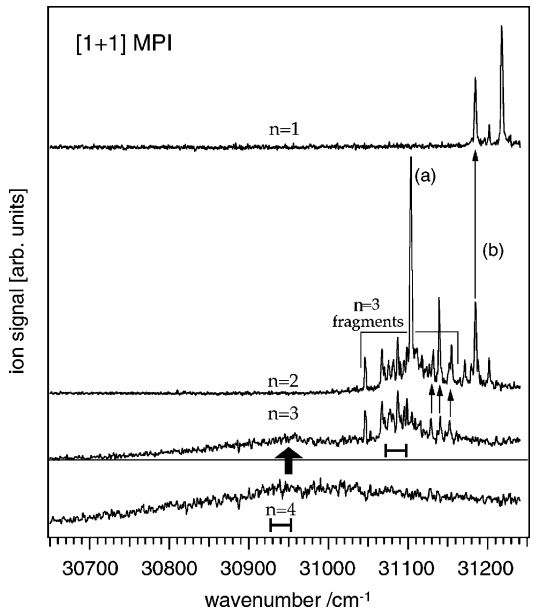

Fig. 3. One-color [1 + 1] MPI-spectra of 1-naphthol/$(NH_3)_n$ clusters. Whereas for $n = 1$–3 structured spectra are obtained, the spectrum of $n = 4$ becomes broad and unstructured. Peaks originating from ionic fragmentation of larger clusters are indicated by arrows. In the ps-experiments a range of states, indicated by horizontal bars, was excited.

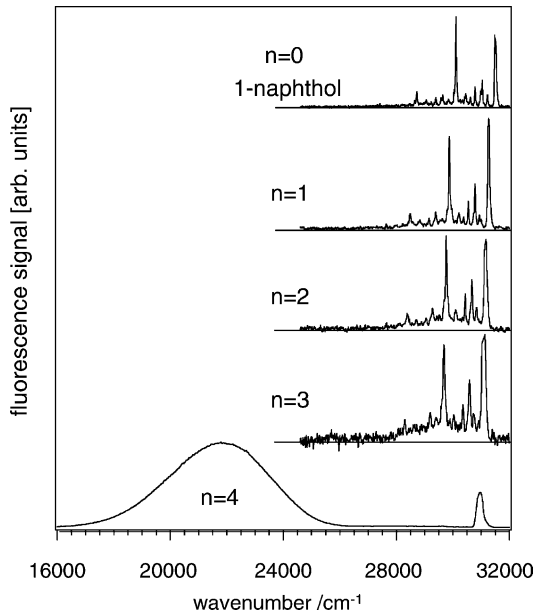

Fig. 4. Laser-induced fluorescence spectra of 1-NpOH/$(NH_3)_n$ clusters. While the spectra obtained upon excitation of the origin bands of the $n = 1$–3 clusters are structured, excitation of the $n = 4$ clusters leads to a fluorescence band red-shifted by more than 8000 cm^{-1}, a clear indication of excited-state proton transfer. Reproduced from [58] by permission of Laser Pages Publishing Ltd.

and Leutwyler reported laser-induced fluorescence (LIF) and one-color [1 + 1] MPI-spectra of 1-NpOH/$(NH_3)_n$ clusters [21]. Their original spectra were similar to those of Fig. 3. Clusters with $n = 1$–3 ammonia molecules show sharp and structured MPI-spectra. The origin of the electronic transition shifts slightly to the red with increasing cluster size ($\Delta\omega < 50\,cm^{-1}/n$), as is usually the case in clusters. However, the appearance of the spectrum changes drastically when the 1-NpOH/$(NH_3)_4$ cluster is monitored. The absorption becomes broad and unstructured, and shifts significantly to the red by several hundreds of wavenumbers.

This change in appearance is also reflected in the emission spectrum (Fig. 4). The various clusters were excited at their origin transitions, and the emission subsequently monitored as a function of wavelength (single vibronic level LIF). Again the clusters with $n = 1$–3 show similar, structured emission spectra. At $n = 4$, on the other hand, the spectrum changes dramatically. The emission spectrum becomes broad and unstructured, its maximum is shifted by 9000 cm^{-1} relative to the excitation wavelength (bottom trace). As discussed above and long known from bulk solution, this broad, red-shifted emission is an indication of excited-state proton transfer in the $n = 4$ cluster.

The appearance of a threshold size for ESPT shows that the relative energy between the first excited covalent state and the charge-separated ion-pair state is modulated by the number of solvent molecules, n. A thermochemical cycle, as depicted in Fig. 5, helps to analyze the various energetic contributions to the overall process. From a thermodynamic point of view, the formation of a solvent-free ion-pair complex is energetically unfavorable, because the absolute values of the gas-phase acidities for the endothermic

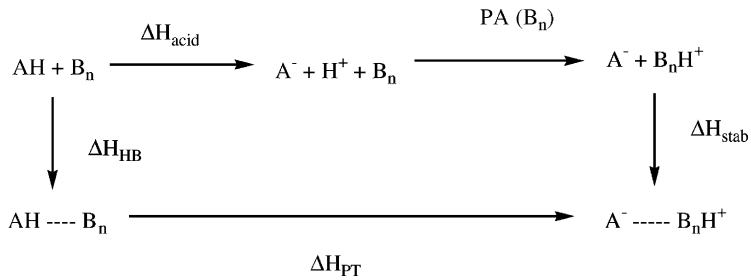

Fig. 5. Whether ESPT is possible for a given cluster size can be determined by use of thermochemical cycles. Since formation of a solvent-free ion-pair complex is endothermic, the sum of the proton affinity PA of the base cluster B_n and the stabilization energy due to charge solvation has to be larger than the gas-phase acidity ΔH_{acid}. In this cycle, ΔH_{HB} is neglected, because it is typically small.

process $HA \rightarrow H^+ + A^-$ are significantly larger than the absolute values of the proton affinities PA for the exothermic process $B_n + H^+ \rightarrow B_nH^+$ [22,23]. However, there is an additional stabilization energy ΔH_{stab}, in clusters due to charge solvation. One can estimate ΔH_{stab} for ESPT in 1-NpOH/$(NH_3)_n$ to be on the order of 90 kcal/mol. Thus, gas-phase proton transfer becomes exothermic only if the proton affinity of the base lies above a certain threshold value. The PA of ammonia clusters increases with cluster size [24]. Thus, when four ammonia molecules surround the photoacid, the proton affinity is high enough (together with the stabilization energy) to move the first excited ion-pair state energetically below the first excited covalent state, ESPT then occurs spontaneously. One has to note, though, that PA and ΔH_{stab} are not independent of each other, since both will depend on the cluster size. Note that the enthalpy of the weak bonds in the cluster, ΔH_{HB}, is typically small and can thus be neglected in the thermochemical analysis.

In order to validate this picture, similar experiments were carried out with other bases as well. When the stronger base piperidine was employed as the solvent [25], the red-shifted emission appeared already at $n = 2$. The PA of two piperidines is close to that of four ammonia molecules (246 vs. 244 kcal/mol [25]), suggesting that for nitrogen bases the straightforward thermodynamic picture is correct. This turns out to reflect adiabatic ESPT. With the weaker bases methanol and water, no clear threshold size was identified for cluster ESPT. As will be discussed below, ESPT in these systems proceeds in a way better described by the non-adiabatic mechanism.

Information on the thermochemistry, but also on the structure of the clusters can be provided by ab initio calculations. For weakly bound ammonia clusters such calculations are possible, but rather difficult [4,26,27]. However, recent calculations discussed ESPT in ammonia clusters of both phenol [28] and naphthol [29]. The computations indicated that ESPT in 1-naphthol/ammonia clusters proceeds exothermic only if at least four ammonia molecules are present to stabilize the excited ammonium naphtholate ion-pair state, in agreement with the experimental data given in this section. The lowest energy covalent structure of the $n = 4$ cluster found in the calculations was a conformer in which the ammonia molecules and the naphthol hydroxyl group form a cyclic structure in both the S_0 and the S_1 state [29].

4. Post-ionization processes

For interpretation of much of the data, it is important to take into account the dissociation mechanisms that are operative. Fragmentation following ionization was examined in particular detail for 1-naphthol/ammonia clusters [30]. The topic has been revisited very recently [31], with somewhat different conclusions, as will be discussed separately below. We first present the “classical” picture.

1-Naphthol/ammonia clusters are readily ionized in one-color MPI experiments which proceed via the S_1 intermediate state. For the $n = 1$ cluster this poses no problems since the cluster is observed to be stable after [1 + 1] photoionization. Already at $n = 2$, however, some fragmentation begins to be observed. Some peaks originating from such these processes are marked by arrows in Fig. 3. The decay pathway is loss of a neutral ammonia molecule in the cluster ion, with a yield of about 50%, as seen in the $n = 1$ mass channel. A similar extent of ion-state fragmentation is observed for all isomers of $n = 3$. These fragmentation pathways are easy to identify since the spectral structure of each cluster size is projected into the next smaller mass channel. That the process occurs in the ion can be readily verified with two-color [1 + 1′] experiments proceeding via the same intermediate states but with less energy in the ionization step. The spectra given in Fig. 6 indicate that the fragmentation process can be suppressed completely. In addition approximate vertical ionization potentials are measured, yielding values of 62,610 cm^{-1} for $n = 0$, near 58,000 cm^{-1} for $n = 1$, 2 and 3, 57,000 cm^{-1} for $n = 4$, and <55,000 cm^{-1} for $n > 4$.

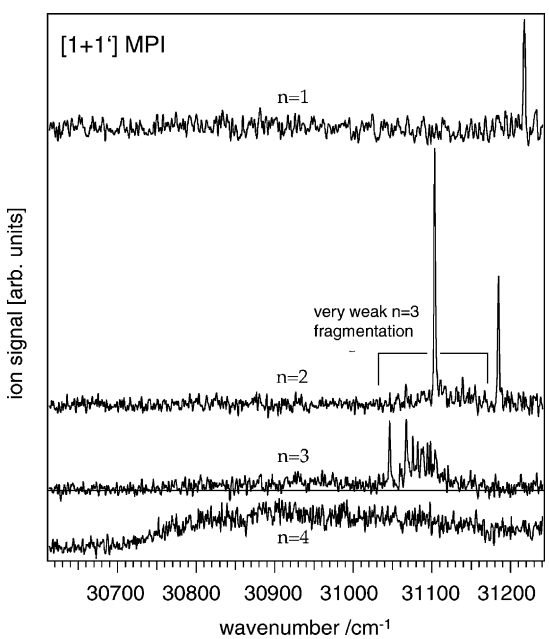

Fig. 6. When MPI-spectra of 1-NpOH/$(NH_3)_n$ clusters are recorded using a two-color [1+1′] scheme, the excess energy in the ion can be reduced, and fragmentation in the ion suppressed. Comparison with the one-color spectra given in Fig. 3 enables identification of the peaks originating from fragmentation in the ion.

By recording a series of spectra over a range of [1+1′] total energies it was found that in a one-color experiment the $n = 4$ cluster fragments with about 30–40% efficiency to $n = 3$, indicated by the broad arrow. As noted in the next section, this is critical for understanding the time-domain results. Above $n = 4$, it is believed that proton transfer occurs already in the ground state [16,21,25]. All these clusters were found to fragment extensively at [1 + 1] photon energies near the $n = 4$ absorption band. Not only are neutral ammonia molecules lost, but there are more complex pathways leading to protonated naphthol/ammonia and ammonia clusters (containing no naphthol). These decay channels are important down to total energies of about 56,000 cm^{-1} for $n = 5$, and even lower for larger clusters.

Two-color experiments have often shown that similar ion-state decay pathways are operative in other naphthol clusters. The usual products are formed by loss of a single solvent molecule. However, the detailed energetics have not been as extensively investigated as for ammonia clusters.

5. Time resolved experiments

Short-pulse spectroscopy in the time-domain is an attractive means to study reactions in clusters, because it has the potential to yield direct information on the reaction time scale [32]. Time-resolved studies on ESPT in both 1-NpOH/solvent [16,33–35] and PhOH/solvent clusters [14,16] were reported soon after the first investigations in the frequency-domain. However, due to the large bandwidths of short pulses it is impossible to excite just one cluster size, rendering time-resolved emission an inconvenient probe method. Instead time-resolved photoionization is generally applied, and all cluster masses are monitored simultaneously. The idea of such an experiment

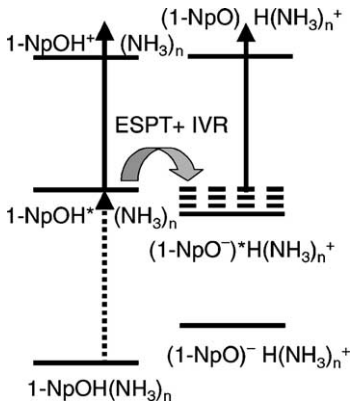

Fig. 7. In time-resolved photoionization experiments, the first excited state is prepared by the pump-photon (dotted arrow). Different parts of the ionic potential energy surface will be accessed upon ionization of the proton-transferred and non-proton-transferred species (full arrows). The change in the ionization cross section leads to a transient in the pump-probe spectra.

is represented in Fig. 7: a pump pulse excites a given cluster to the first excited covalent state (dotted arrow), a time-delayed probe pulse (solid arrow) ionizes the cluster. If a certain cluster undergoes ESPT during the delay time (curved arrow), it will be ionized from the proton-transferred state, with excitation terminating in the proton-transferred state of the ion. If the cluster does not undergo ESPT, ionization will occur from the excited covalent state and terminate in the non-proton-transferred state of the ion. In this simple picture, motion from the non-proton transferred to the proton-transferred part of the excited state surface will lead to a time-dependent pump-probe signal, because the character of the intermediate state changes.

However, two issues have to be considered carefully. First, a transient in a pump-probe photoionization spectrum only reflects a change in the ionization cross section due to the evolution of the intermediate state wavepacket during the course of the experiment. What set of phenomena cause this change, however, is a matter of interpretation. As discussed in connection with the potential curves in Fig. 2, IVR and solvent reorganization will contribute in addition to ESPT to the overall dynamics of the process, and might also lead to a time-dependent ionization cross section. In phenol/ammonia clusters in addition transfer of hydrogen atoms presumably contributes to the transient observed in short-pulse experiments [19]. Therefore, time-resolved photoionization is a less direct probe of ESPT than time-resolved emission. Second, as discussed in the preceding section, photoionization experiments in both, time- and frequency-domain, can be obscured by cluster fragmentation in the ion, because part of the signal observed in a given mass channel might originate from a larger cluster and thus carries the signature of its dynamics. Since selective excitation of a given cluster mass is difficult due to the large frequency bandwidth, cluster fragmentation is a more severe problem in short-pulse experiments than in high-resolution experiments.

The first issue can be solved by utilizing both the time- and frequency-domain information. In the case of ESPT in 1-naphthol/solvent clusters, much high-resolution data is available as a basis for the time-resolved studies. In order to treat the second issue appropriately, photoionization spectra in the time-domain, as in the frequency-domain, must be recorded at low excess energy in the ion to minimize the contribution of fragments.

In a recent publication, we reported time-resolved pump-probe photoionization spectra of 1-NpOH/$(NH_3)_n$ clusters as a function of wavelength [36], employing independently tunable 2.5 ps pulses, provided by two optical parametric generators. The details of the experimental setup were described elsewhere [37]. Two different excitation wavelengths were chosen, 321.7 (31,085 cm^{-1}) and 323.2 nm (30,940 cm^{-1}), giving maximum signals in the $n = 3$ and $n = 4$ channels, respectively. Owing to the 25 cm^{-1} bandwidth of the ps-pulses a range of vibrational states is excited, indicated by the horizontal bars in Fig. 3. Since the excitation energy generally shifts to the red with increasing cluster size, contributions from larger clusters will always be present. We minimized them by working at very low concentrations of both 1-naphthol and ammonia, and by working early in the gas pulse. Signals were recorded for all mass channels ranging from $n = 0$ to $n = 6$, but transients were only observed in the $n = 3$ and $n = 4$ mass channels.

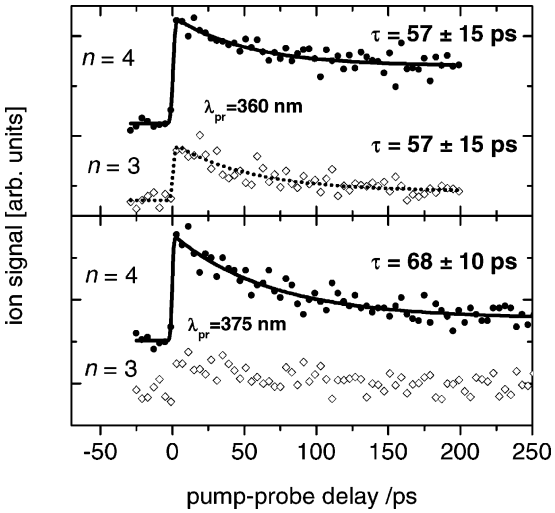

Fig. 8. Decay dynamics in the 1-naphthol/$(NH_3)_n$, $n = 3$ and 4, clusters, excited at 30,940 cm^{-1}, as a function of probe wavelength. Going from 27,780 cm^{-1} (upper trace) to 26,670 cm^{-1} (lower trace) reduces the amount of excess energy deposited in the cluster ions from 2700 to 1600 cm^{-1}. The signal in the $n = 3$ mass channel disappears almost completely, confirming that it originates from ammonia evaporation in the $n = 4$ cluster ion. By comparison with the frequency-domain results, the transient in the $n = 4$ channel was assigned to excited-state proton transfer, associated with IVR and solvent reorganization. Reproduced from [36] by permission of the Royal Society of Chemistry on behalf of the PCCP owner societies.

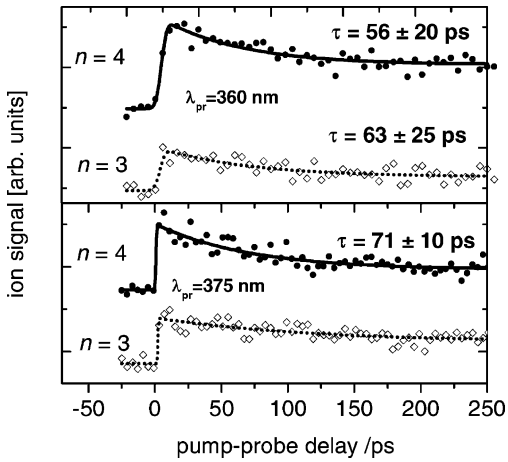

Fig. 9. Decay dynamics in the 1-naphthol/$(NH_3)_n$, $n = 3$ and 4, clusters, excited at 31,085 cm^{-1}, as a function of probe wavelength. The transient in the $n = 4$ mass channel becomes more pronounced upon going from 27,780 cm^{-1} (upper trace) to 26,670 cm^{-1} (lower trace). In contrast, the transient in the $n = 3$ channel disappears almost completely and shows only a nanosecond time dependence. Reproduced from [36] by permission of the Royal Society of Chemistry on behalf of the PCCP owner societies.

Two probe wavelengths were utilized, 360 nm (27780 cm^{-1}) and 375 nm (26670 cm^{-1}). The resulting time-delay scans are depicted in Figs. 8 and 9. At a pump wavelength of 323.2 nm (Fig. 8) only the $n \geq 4$ cluster is excited. However, time-delay scans recorded at a probe wavelength of 360 nm show time-dependent transients in both mass channels, $n = 3$ and $n = 4$, with a similar lifetime of 57 ps. In the preceding section, we already discussed the loss of an ammonia unit in the cluster cation. The binding energy of 2680 cm^{-1} that has been determined for the neutral ground state [38] of 1-NpOH/$(NH_3)_1$ can serve as a rough estimate for the binding energy in the ion. Considering that an excess energy of around 2900 cm^{-1} is deposited in the $n = 4$ ion in the probe step, and taking the information on post-ionization processes from ns-experiments into account, fragmentation in the ion is likely to be the origin of the transient in the $n = 3$ channel.

When the probe wavelength is reduced to 375 cm^{-1}, corresponding to an excess energy of only 1600 cm^{-1} in the $n = 4$ ion, the transients depicted in the lower part of Fig. 8 were obtained. While the transient in $n = 4$ channel is even more pronounced, the transient in the $n = 3$ channel has almost completely disappeared, confirming the $n = 3$ transient at $\lambda_{probe} = 360$ nm to be caused by fragmentation in the $n = 4$ cluster ion. In agreement with the frequency-domain results, the transient in the $n = 4$ channel is assigned to formation of the proton-transferred ion-pair state. However, it must be kept in mind that the time constant of ≈60 ps corresponds to a complicated motion along the excited state surface, including not only proton transfer, but also IVR and solvent reorganization. For example, recent calculations on the phenol/ammonia system [28] indicate that the solvent molecules reorganize almost instantaneously as the proton transfer progresses.

The picture was confirmed by experiments at a pump wavelength of 321.7 nm, exciting both the $n = 3$ and the $n = 4$ cluster (Fig. 9). Again, at $\lambda_{probe} = 360$ nm transients are visible in both mass channels.

When the excess energy in the ion is reduced by probing at 375 nm, the $n = 4$ transient is still present, whereas no fast dynamics is visible in the $n = 3$ channel.

6. 1-Naphthol/water clusters

The ESPT behavior of 1-naphthol in water clusters is distinctly different from that in ammonia clusters. The LIF spectra obtained under various expansion conditions are given in Fig. 10, together with the mass spectra, showing the corresponding cluster size distribution. A red-shifted naphtholate fluorescence is also observed, but only for cluster sizes greater than about 25 [25,39,40,41], significantly larger than in 1-naphthol/ammonia clusters. A precise size threshold may not exist, and is anyway not readily determined because of the unavoidable congestion of the excitation spectra in this size range.

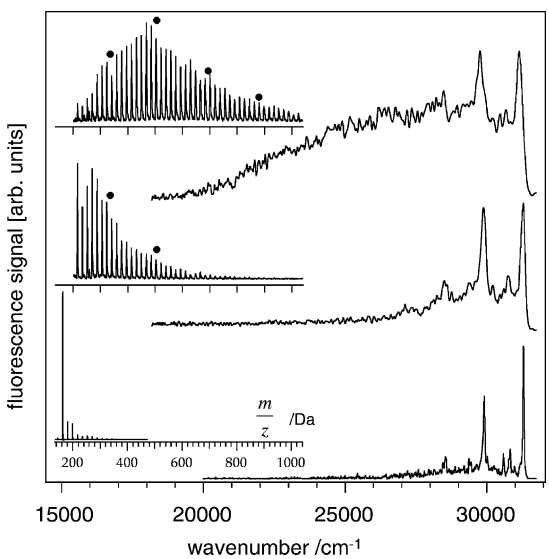

Fig. 10. Laser-induced fluorescence spectra of 1-naphthol/$(H_2O)_n$ clusters under different expansion conditions. The corresponding mass spectra are shown as insets in the figure, the filled circles indicate clusters with $n = 10, 20, 30 \ldots$. The LIF spectra change only gradually, no clear threshold size for ESPT is visible. The excitation frequencies were from bottom to top 31,311 cm^{-1} ($n = 1$ origin), 31,280 and 31,153 cm^{-1}. Reproduced from [58] by permission of Laser Pages Publishing Ltd.

The PA of an $n = 25$–30 water aggregate is in the correct range to induce ESPT, according to the thermodynamic model. The adiabatic picture is, however, unable to account for several other observations made on this system. Remarkably, the naphtholate fluorescence for a given cluster distribution was found to be dependent on the degree of cooling in the molecular beam. For warmer clusters more naphtholate fluorescence was present. The spectrum was also observed to shift to lower energy over time scales of 5–20 ns. Colder clusters showed no such evolution, and narrower spectra [39,40]. Interestingly, the red-shift was also more pronounced in the warmer spectra.

In contrast to ammonia clusters, the naptholate fluorescence rise time, and hence the ESPT time scale, is readily measured. There are fast (<60 ps), intermediate (1 ns) and slow (several ns) components to the emission. This is partly because a range of cluster sizes are always excited, but the size dependence of the rate is not as might be expected. Even though the PA of the cluster increases with size, the rate *decreases* for larger clusters [41].

The slow ESPT, size and "temperature" dependence of the rate, and the post-ESPT spectral relaxation all point to a non-adiabatic reaction mechanism. The current picture is that the S_1 is much like the L_b of the uncomplexed naphthol. The new electronic configuration induces solvent rearrangement around the chromophore, which in turn stabilizes an increasingly polar excited state, i.e. an increasing amount of L_a character is mixed into the L_b state. This process is self-reinforcing, leading, in larger clusters, finally to inversion of the states and ESPT. Its rate is limited by solvent motion, which is why the sizes and temperatures of the clusters are so important.

The temperature effect is clear, but the size effect is less familiar. Finite systems have phase transition temperatures that are lower than those of bulk (infinite) systems. The temperature width of the transition also becomes finite, so there is no well-defined melting or freezing point [42]. Clusters may therefore be considered "slushy," and the amount and rate of intermolecular motion is dependent on the cluster internal energy. Larger clusters will be more bulk-like at

the same temperature. In the case of 1-naphthol/water this means the largest clusters with the highest PA are more similar to ice than the smaller ones, and therefore should exhibit slower internal motion. This is exactly what is observed for the ESPT rate as well as the post-ESPT relaxation. Could even larger clusters be generated than the 800–1000 already attained, it is expected that ESPT would stop, since it is not observed for 1-naphthol in bulk ice [43].

An important remaining aspect of ESPT in water and water clusters is that of the feedback mechanism that starts the process. The L_b state of 1-naphthol is not much more polar than the ground state, so it should not induce much solvent reorganization. However, it was found that certain vibrational modes of free 1-naphthol mix the L_a and L_b states [44]. In a cluster with one water, vibronic coupling was enhanced [45]. Calculations of naphthol in water show that this is indeed sufficient to trigger solvent rearrangement, and start the process of level inversion and ESPT [44]. Vibronic state mixing in 1-naphthol was also experimentally verified by high resolution rotational spectroscopy [46].

7. Comparison with other naphthols

7.1. 2-Naphthol

2-Naphthol is an obvious candidate for comparison with 1-naphthol. It is a slightly weaker excited state acid (pK_a^* 2.8 vs. 0.4, in water), but in the gas phase the acidity difference is less than the PA difference between 4 and 5 ammonia molecules. As a result the size threshold for ESPT in ammonia clusters is also $n = 4$ [47], and therefore, consistent with the thermodynamic model developed for 1-naphthol. Although less well studied, all indications from nanosecond MPI and LIF experiments are that the reaction is also adiabatic in nature.

In bulk water, the 2-naphthol ESPT reaction is activated (2.6 kcal/mol), and therefore, unable to compete with other decay pathways even at temperatures above 0 °C [48]. Consistent with this, no ESPT was observed in water clusters, even when attempts were made to warm them somewhat [39,40]. In contrast to 1-naphthol, there is at present no evidence for an excited state inversion prior to proton transfer in water solutions of 2-naphthol [49].

7.2. 5-Cyano-2-naphthol

The excited-state acidity of aromatic systems is increased upon addition of electron-withdrawing substituents that can stabilize the charge-separated state. 5-Cyano-2-naphthol is one member of a family of such "super" photoacids that have recently been developed in order to study the effect of electron-withdrawing substituents on ESPT dynamics [50–53]. Due to its greater acidity ($pK_a^* = -0.3$ in water [53]) as compared to 1-naphthol, ESPT from 5-cyano-2-naphthol is observed not only in water, but also in solvents such as methanol or DMSO [52,53].

From the LIF spectra depicted in Fig. 11 the size threshold for ESPT in ammonia clusters was concluded to be either 3 or 4. Because the MPI excitation spectra become unstructured above $n = 1$, a more precise threshold could not be established. The increment in excited state acidity compared to 1-naphthol is approximately −5 kcal/mol, slightly smaller than the PA differences between $(NH_3)_3$ and $(NH_3)_4$ (8 kcal/mol), so either threshold is compatible with the thermodynamic and adiabatic models. On the other hand, the strongly red-shifted naphtholate emission was observed to appear with a time delay comparable to the molecular emission (2–3 ns), suggesting either a slow (non-adiabatic?) ESPT reaction or post-ESPT relaxation. This remains to be studied in more detail.

Clusters of 5-cyano-2-naphthol with water were found to be rather similar to 1-naphthol/water clusters in their ESPT behavior [54]. In accordance with the greater acidity the size threshold is smaller for 5-cyano-2-naphthol, ESPT appears already at $n \approx 10$ as compared to 25–30 in 1-naphthol, but otherwise some of the same effects were observed. In particular, the extent of ESPT is dependent on the temperature of the clusters, as is the red-shift of the naphtholate emission. The anion emission is also delayed

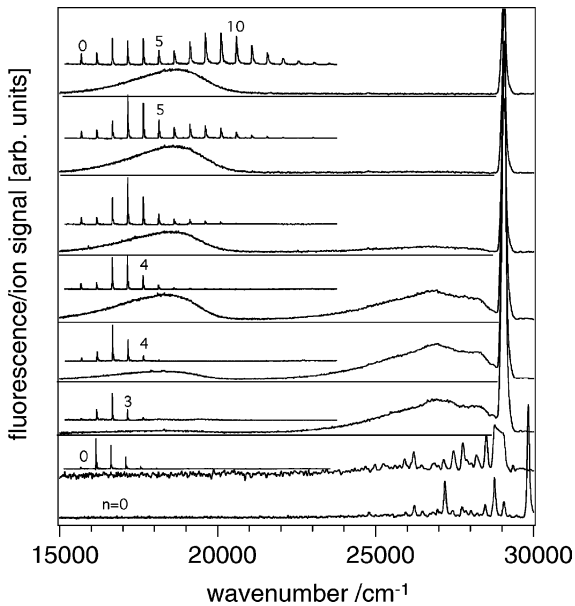

Fig. 11. Laser-induced fluorescence spectra of 5-cyano-2-naphthol/$(NH_3)_n$ clusters under different expansion conditions, with the corresponding mass spectra shown in the insets. The red-shifted ESPT emission appears when $n = 3$ and $n = 4$ clusters are present in the jet. A clear threshold size cannot be given, because the absorption spectra are unstructured for all $n > 1$, preventing selective cluster excitation. The clusters were excited at 29,826 cm^{-1} (bottom most trace, $n = 0$), 28,882 cm^{-1} ($n = 1$) and 29,100 cm^{-1} (all other spectra), and ionized at 36,350 cm^{-1}. Reprinted with permission from [54]. Copyright (2001) American Chemical Society.

by a few nanoseconds with respect to the unreacted naphthol fluorescence. All these data point to a non-adiabatic model in which solvent reorganization around the chromophore is a key part of the reaction pathway.

In contrast to the above two cases, 5-cyano-2-naphthol clustered with methanol or a mixture of methanol and water was not observed to undergo ESPT at all. This in spite of the fact that the reaction occurs in bulk methanol solution. With increasing cluster size the fluorescence shifts moderately to the red, but never gives any indication of a break to a naphtholate-like emission as known from the bulk. Since the pK_a^* in methanol is 2.6 [53], well above zero, the difference in cold clusters vs. bulk is, as for 2-naphthol/water, attributable to thermal activation. In clusters the temperature is so low that enthalpic effects are dominant, while entropy plays a more significant role in bulk media at room temperature. This provides an excellent example of how experimentally observed differences between cluster and bulk phase behavior enhance our understanding of ESPT in bulk media, in this case by judging the relative importance of enthalpic and entropic factors.

8. Understanding the differences in ESPT behavior

The existing data are now sufficiently extensive that we can begin to develop some general ideas regarding factors determining ESPT in naphthol/solvent clusters.

The proton affinity of the solvent cluster is clearly important, and can be estimated from that of the corresponding naphthol-free solvent cluster. This is because, at least for smaller clusters, the solvent molecules form a compact hydrogen bonded "nanodroplet" attached to the hydroxyl group of the naphthol [26,55–57]. In several cases, the PA has high predictive value for the ESPT size threshold, but this appears only to be true when the reaction is adiabatic in nature. More precisely, the proton withdrawing or accepting strength of the solvent seems to be a significant determinant of the reaction type. Strong proton acceptors, such as the nitrogen bases, appear to be effective in inducing pre-excitation L_a/L_b state mixing, leading to adiabatic ESPT. For weaker proton acceptors, such as the oxygen bases, the excited states appear to remain more similar to the uncomplexed molecule, prior to excitation. The post-excitation processes then needed for ESPT are described as non-adiabatic.

These non-adiabatic dynamic events seem to depend considerably on direct interaction of the solvent with the aromatic ring, and not just the hydroxyl group. This can be partly understood in terms of better proton back-donation characteristics of the oxygen bases to the nascent extended anion. There also seems to be a need for substantial ring interaction, because the solvent-induced post-excitation L_a/L_b state mixing is

enabled by vibronic coupling with vibrational modes corresponding to motion of the ring atoms. This process involves orientational motions of the solvent and is therefore, sensitive to the internal energies of the clusters.

The ESPT time scales depend on the reaction type. Adiabatic ESPT is relatively fast, but is limited by the IVR-like evolution of the wave packet into many degrees of freedom. This point is important, since the rate in a single effective coordinate model is on the order of the vibrational frequency, and thus too fast. ESPT in these systems might be understood in terms of multi-tier IVR, branching into increasingly many coordinates as the reaction progresses. The time-dependent transients then reflect not only the actual proton motion but also many associated motions. Nevertheless a single effective proton transfer coordinate model can serve as a first approximation, albeit a rather crude one.

In the non-adiabatic case, the "ESPT rate" is more a measure of the solvent orientational adaptation to the electronic state, and the progress of the electronic/solvent relaxation process. At some point along the way, the proton is transferred, and relaxation continues. Separation of the proton jump from the rest is not straightforward, and a single effective coordinate model becomes a questionable approximation.

9. Fragmentation revisited and a new ESPT model

From the information summarized above a coherent picture of the excited-state proton transfer in naphthol/solvent clusters has been developed. However, recent experiments on the fragmentation dynamics in 1-naphthol/ammonia clusters by Dedonder-Lardeux et al. suggest that an alternative interpretation might be possible [31]. This group utilizes the fact that upon fragmentation in the cluster ion, i.e. evaporation of an ammonia unit, part of the excess energy is released as translational energy, leading to a broadening of the daughter ion peak in the time-of-flight mass spectrum. As an example, we will discuss the results obtained upon optical excitation of the bands assigned as (a) and (b) in Fig. 3. Fig. 12 shows the TOF mass spectra obtained upon resonant (solid line) and off-resonant (dotted line) excitation in the upper trace, the difference spectrum is shown in the lower trace. The off-resonance spectrum was recorded to take background contributions into account, thus, the difference spectrum represents the "true" mass spectrum for the respective excitation. As visible in the left hand trace, upon excitation of band (a) only the 1-NpOH/$(NH_3)_2^+$ cluster appears in the mass spectrum, whereas both, the $n = 2$ and $n = 1$ cluster appear upon excitation

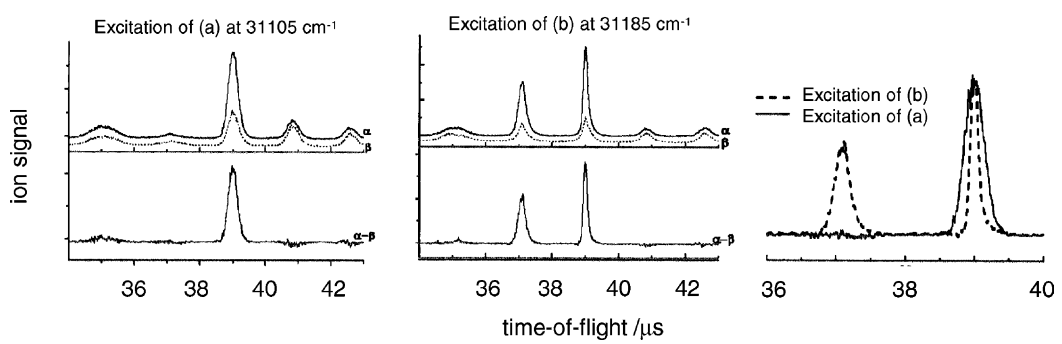

Fig. 12. Information on fragmentation in the ion can be obtained from an analysis of the translational energy release in the [1 + 1] MPI-spectra. The figure shows TOF mass spectra obtained upon excitation of the bands marked (a) and (b) in Fig. 3. The off-resonance spectra marked β where taken to correct for background contributions. Upon excitation of band (a) only the $n = 2$ cluster appears in the mass spectrum (left-hand side), while both, $n = 1$ and 2 appear upon excitation of (b). An analysis of the translational energy release (right-hand side) reveals that not only the $n = 1$ band obtained by excitation of (b) but also the $n = 2$ band obtained upon excitation of (a) are due to fragmentation in the ion. The occurrence of this band demonstrates that some clusters undergo 100% fragmentation in the ion. Reproduced from [31] by permission of the Royal Society of Chemistry on behalf of the PCCP owner societies.

of the (b) band (center trace). One might thus conclude that band (b) represents excitation of the $n = 2$ cluster, which loses an ammonia unit and fragments into the $n = 1$ channel, while band (a) represent an excitation of the $n = 2$ cluster that does not lead to fragmentation due to the smaller excess energy. However, this interpretation becomes questionable when the kinetic energy release is taken into account, as visible in the right-hand trace of Fig. 12. The dashed line corresponds to excitation of band (b), the solid line to excitation of (a). Excitation of (b) leads to a narrow mass peak in the $n = 2$ channel, but to a broadened peak in the $n = 1$ channel. The broadening is due to the translational energy gained upon fragmentation in the ion. Excitation of (a), on the other hand, leads to a peak in the $n = 2$ channel that is significantly broader as compared to the peak obtained upon excitation of (b). In fact, its width is comparable to the $n = 1$ fragment peak observed upon excitation of (b), suggesting that it originates from fragmentation as well. The proposed explanation for this observation is a fragmentation of the $n = 3$ cluster ion that occurs with almost 100% efficiency. A possible reason for the efficient fragmentation suggested in this paper is that in all cluster ions $n \geq 2$ the proton transferred structure is the most stable. Since proton transfer in the ion is exothermic, a lot of energy is released, leading to extensive fragmentation. In phenol/ammonia clusters, for example, proton transfer in the ion was found to proceed rapidly and without any significant barrier [59] even in the $n = 1$ cluster. As a consequence, 1-naphthol/$(NH_3)_n$ clusters with $n = 3$ and $n = 4$ might also fragment with 100% yield in the ion, suggesting that the ESPT dynamics observed for the $n = 4$ cluster is rather due to the $n = 5$ cluster.

This is, however, apparently in conflict with the time-domain results. We discussed how the dynamics of the mass channel n can appear in the $n - 1$ channel due to fragmentation in the ion, but it should also be apparent in the channel n. In the time-domain experiments no time-dependence was observed in the $n = 5$ channel. In order to address this problem, Dedonder-Lardeux et al. developed a model that considers fragmentation in the excited state of the neutral clusters in addition to fragmentation in the ion: the observed transient at the mass corresponding to n ammonia units is suggested to be a sum of four reaction channels: (1) the $n + 2$ cluster, losing two ammonia units due to fragmentation in the ion, (2) the $n+2$ cluster losing one ammonia in the neutral excited state and another ammonia in the ion, (3) the $n + 1$ cluster losing one NH_3 in the ion, and (4) the $n+1$ cluster losing one unit in the neutral excited state. As an example, let us consider the influence of processes occurring in the $n = 6$ cluster on the signal in the $n = 5$ channel, i.e. reaction channels (3) and (4). The $n = 6$ cluster loses an ammonia unit in the intermediate state; this leads to a decreasing ionization yield with time and thus to decreasing fragmentation in the ion. In turn the signal in the $n = 5$ channel, which reflects the $n = 6$ dynamics, becomes smaller with time. On the other hand, fragmentation in the $n = 6$ *neutral* intermediate state results in neutral $n = 5$ clusters and subsequently increases the signal in this mass channel. One might thus end up with a pump-probe spectrum showing no time-dependence. Within this picture a transient in the $n = 4$ channel appears because fragmentation in the $n = 5$ neutral is suppressed, and thus a channel leading to an increase in signal is turned off, whereas the channels leading to a decrease of signal, evaporation of an ammonia unit in the $n = 5$ cation being one of them, remain open. If this was true, the transients would not reflect ESPT dynamics at all, but only fragmentation dynamics. Using reasonable boundary conditions and assumptions for some parameters, some aspects of the time-dependent transients were simulated quite well. At the same time, it is not clear that all important features can be reproduced. For example, the deep transient found on $n = 4$ at the lowest $[1 + 1']$ energies may be difficult to explain. Also key assumptions about excess energy and fragmentation rates in the S_1 state of larger clusters have yet to be confirmed.

The model, thus, constitutes a consistent but not confirmed alternative explanation for much of the data. Correctly, it looks closely at processes that were insufficiently considered by earlier authors. While it does represent a revision of the overall picture, its main

effect is not to invalidate the earlier conclusions, but to shift the existing interpretation one unit to larger size. However, in order to validate the model, additional experiments need to be carried out, including $[1+1']$ two-color ionization studies of the kinetic energy release at various excess energies in the ion.

10. Summary and conclusions

In this review, we have summarized the experimental data on excited-state proton transfer in 1-naphthol/$(NH_3)_n$ clusters. $[1+1]$ MPI-spectra yield structured spectra for clusters with $n = 1$–3 ammonia units, but a broad and unstructured spectrum for the $n = 4$ clusters. In laser-induced fluorescence spectra a broad and red-shifted emission appears that resembles the emission observed in aqueous solution and indicates excited-state proton transfer. Two-color $[1+1']$ MPI-spectra reveal that significant fragmentation occurs in the cluster ions. From time-domain spectra, recorded by picosecond time-resolved photoionization, a decay with a time constant of 50 ps is obtained for the $n = 4$ cluster. This time constant is assigned in the classical picture to a complicated motion on a multidimensional surface that includes not only ESPT but also IVR and solvent reorganization.

ESPT to nitrogen containing bases is best described by an adiabatic model. Within this model the electronic states of the naphthol-chromophore are strongly coupled and proton transfer proceeds on a single electronic surface. ESPT to oxygen-containing bases, like water or methanol, is better described within a non-adiabatic model, with the electronic states of naphthol largely retaining their original character. Proton transfer occurs because of state mixing induced by vibronic coupling during the reaction, due to reorganization of the solvent. This leads finally to an inversion of states, enabling proton transfer. The picture is confirmed by experiments on the closely related chromophores 2-naphthol and 5-cyano-2-naphthol.

While the assumption of a single proton-transfer coordinate in the adiabatic mechanism is an oversimplification, it can serve as a crude first approximation. In the non-adiabatic case, on the other hand, the use of a single effective proton transfer coordinate appears inappropriate.

Also briefly reviewed is a new model for ESPT from 1-naphthol to ammonia by the Orsay group. It takes into account a variety of S_1 and ion state fragmentation and proton transfer processes. Certain aspects need to be confirmed by further experiments, but it clearly represents very useful new thinking. If correct, the size threshold for ESPT in this system is at five ammonia molecules, rather than four.

Acknowledgements

The authors would like to thank Christophe Jouvet (Orsay) for numerous discussion on excited-state proton transfer.

References

[1] T.D. Märk, A.W. Castleman Jr., Adv. Atom. Mol. Phys. 20 (1985) 65.
[2] K. Müller-Dethlefs, P. Hobza, Chem. Rev. 100 (2000) 143.
[3] C. Desfrançois, C. Carles, J.P. Schermann, Chem. Rev. 100 (2000) 3943.
[4] P.E.S. Wormer, A. van der Avoird, Chem. Rev. 100 (2000) 4109.
[5] G. Chalasinski, M.M. Szczesniak, Chem. Rev. 100 (2000) 4227.
[6] Q. Zhong, A.W. Castleman Jr., Chem. Rev. 100 (2000) 4039.
[7] E.M. Kosower, D. Huppert, Ann. Rev. Phys. Chem. 37 (1986) 127.
[8] C.R. Moylan, J.I. Brauman, Annu. Rev. Phys. Chem. 34 (1982) 187.
[9] N.F. Scherer, L.R. Khundkar, R.B. Bernstein, A.H. Zewail, J. Chem. Phys. 87 (1987) 1451.
[10] S.I. Ionov, G.A. Brucker, C. Jaques, J.L. Valachovic, C. Wittig, J. Chem. Phys. 97 (1992) 9486.
[11] S.I. Ionov, G.A. Brucker, C. Jaques, L. Valachovic, C. Wittig, J. Chem. Phys. 99 (1993) 6553.
[12] T. Förster, Z. Elektrochem. 54 (1950) 531.
[13] A. Weller, Z. Elektrochem. 56 (1952) 662.
[14] J. Steadman, J.A. Syage, J. Chem. Phys. 92 (1990) 4630.
[15] J.A. Syage, J. Steadman, J. Chem. Phys. 95 (1991) 2497.
[16] S.K. Kim, J.J. Breen, D.M. Willberg, L.W. Peng, A. Heikal, J.A. Syage, A.H. Zewail, J. Phys. Chem. 99 (1995) 7421.
[17] S. Martrenchard-Barra, C. Dedonder Lardeux, C. Jouvet, D. Solgadi, M. Vervloet, G. Gregoire, I. Dimicoli, Chem. Phys. Lett. 310 (1999) 173.

[18] G. Pino, C. Dedonder-Lardeux, G. Grégoire, C. Jouvet, S. Martrenchard, D. Solgadi, J. Chem. Phys. 111 (1999) 10747.
[19] G. Pino, G. Grégoire, C. Dedonder-Lardeux, C. Jouvet, S. Martrenchard, D. Solgadi, Phys. Chem. Chem. Phys. 2 (2000) 893.
[20] D. Borgis, J.T. Hynes, J. Phys. Chem. A 100 (1996) 1118.
[21] O. Cheshnovsky, S. Leutwyler, J. Chem. Phys. 88 (1988) 4127.
[22] D.H. Aue, M.T. Bowers, in: M.T. Bowers (Ed.), Gas-Phase Ion Chemistry, Academic Press, New York, 1979, p. 2.
[23] J.E. Bartmess, R.T. McIver Jr., in: M.T. Bowers (Ed.), Gas-Phase Ion Chemistry, Academic Press, New York, 1979, p. 88.
[24] J.D. Payzant, A.J. Cunningham, P. Kebarle, Can. J. Chem. 51 (1973) 3242.
[25] R. Knochenmuss, O. Cheshnovsky, S. Leutwyler, Chem. Phys. Lett. 144 (1988) 317.
[26] Y. Matsumoto, T. Ebata, N. Mikami, J. Mol. Struct. 552 (2000) 257.
[27] D. Henseler, C. Tanner, H.M. Frey, S. Leutwyler, J. Chem. Phys. 115 (2001) 4055.
[28] W. Siebrand, M.Z. Zgierski, Z.K. Smedarchina, Chem. Phys. Lett. 279 (1997) 377.
[29] W. Siebrand, M.Z. Zgierski, Chem. Phys. Lett. 320 (2000) 153.
[30] R. Knochenmuss, Chem. Phys. Lett. 311 (1999) 439.
[31] C. Dedonder-Lardeux, D. Grosswasser, C. Jouvet, S. Martrenchard, A. Teahu, Phys. Chem. Chem. Phys. 3 (2001) 4316.
[32] A.H. Zewail, Femtochemistry, World Scientific, Singapore, 1994.
[33] J.J. Breen, L.W. Peng, D.M. Willberg, A. Heikal, P. Cong, A.H. Zewail, J. Chem. Phys. 92 (1990) 805.
[34] M.F. Hineman, D.F. Kelley, E.R. Bernstein, J. Chem. Phys. 97 (1992) 3341.
[35] S.K. Kim, J.K. Wang, A.H. Zewail, Chem. Phys. Lett. 228 (1994) 369.
[36] D.C. Lührs, R. Knochenmuss, I. Fischer, Phys. Chem. Chem. Phys. 2 (2000) 4335.
[37] T. Schultz, J.S. Clarke, H.-J. Deyerl, T. Gilbert, I. Fischer, Faraday Discuss. 115 (2000) 17.
[38] T. Bürgi, T. Droz, S. Leutwyler, Chem. Phys. Lett. 246 (1995) 291.
[39] R. Knochenmuss, D.E. Smith, J. Chem. Phys. 101 (1994) 7327.
[40] R. Knochenmuss, J. Chim. Phys. PC B 92 (1995) 445.
[41] R. Knochenmuss, G.R. Holtom, D. Ray, Chem. Phys. Lett. 215 (1993) 188.
[42] P.Z. Pawlov, Phys. Chem. 65 (1909) 545.
[43] R. Knochenmuss, S. Leutwyler, J. Chem. Phys. 91 (1989) 1268.
[44] R. Knochenmuss, P.L. Muino, C. Wickleder, J. Phys. Chem. 100 (1996) 11218.
[45] R. Knochenmuss, V. Karbach, C. Wickleder, S. Graf, S. Leutwyler, J. Phys. Chem. A 102 (1998) 1935.
[46] S.J. Humphrey, D.W. Pratt, Chem. Phys. Lett. 257 (1996) 169.
[47] T. Droz, R. Knochenmuss, S. Leutwyler, J. Chem. Phys. 93 (1990) 4520.
[48] G.W. Robinson, P.J. Thistlethwaite, J. Lee, J. Phys. Chem. 90 (1986) 4224.
[49] B.Z. Magnes, N.V. Strashnikova, E. Pines, Isr. J. Chem. 39 (1999) 361.
[50] L.M. Tolbert, J.E. Haubrich, J. Am. Chem. Soc. 116 (1994) 10593.
[51] K.M. Solntsev, D. Huppert, L.M. Tolbert, N. Agmon, J. Am. Chem. Soc. 120 (1998) 7981.
[52] K.M. Solntsev, D. Huppert, N. Agmon, J. Phys. Chem. A 102 (1998) 9599.
[53] K.M. Solntsev, D. Huppert, N. Agmon, J. Phys. Chem. A 103 (1999) 6984.
[54] R. Knochenmuss, K.M. Solntsev, L.M. Tolbert, J. Phys. Chem. A 105 (2001) 6393.
[55] R. Yoshino, K. Hashimoto, T. Omi, S. Ishiuchi, M. Fuji, J. Phys. Chem. A 102 (1998) 6227.
[56] S. Ishiuchi, M. Sakai, K. Daigoku, T. Ueda, T. Yamanaka, K. Hashimoto, M. Fuji, Chem. Phys. Lett. 347 (2001) 87.
[57] Y. Matsumoto, T. Ebata, N. Mikami, J. Phys. Chem. A 105 (2001) 5727.
[58] R. Knochenmuss, I. Fischer, D. Lührs, Q. Lin, Isr. J. Chem. 39 (1999) 221.
[59] H.-T. Kim, R.J. Green, J. Quian, S.L. Anderson, J. Chem. Phys. 112 (2000) 5717.